

Study of the conversion of N-carbamoyl-L-proline to hydantoin-L-proline using powder synchrotron X-ray diffraction

Luis E. Seijas, Asiloé J. Mora,^{a)} and Gerzon E. Delgado^{b)}

Laboratorio de Cristalografía, Departamento de Química, Facultad de Ciencias, Universidad de Los Andes, Mérida 5101, Venezuela

Michela Brunelli

Institut Laue Langevin, BP 156, F-38042 Grenoble Cedex, France

Andrew N. Fitch

European Synchrotron Radiation Facility, BP 220, F-38043 Grenoble Cedex, France

(Received 27 May 2010; accepted 10 August 2010)

The solvent-free conversion of N-carbamoyl-L-proline to hydantoin-L-proline by direct heating at 470 K is reported. A reaction mechanism is proposed based on a nucleophilic intramolecular substitution reaction involving both the lone pair of the NH₂ group and the carboxylic acid group of the N-carbamoyl-L-proline. The DSC and TGA experiments show rising of the baselines of the curves prior to melting and decomposition given evidence of the onset of the thermal reaction. NMR experiments were used to identify the product of the reaction, hydantoin-L-proline, whose crystal structure was obtained from X-ray synchrotron powder diffraction data collected on the solidified melt. This compound displays a crystal packing directed by hydrogen bonds forming a layered structure pile up along the *c* direction. © 2010 International Centre for Diffraction Data. [DOI: 10.1154/1.3503660]

Key words: hydrogen bonding, hydantoin, crystal structure, X-ray powder diffraction, synchrotron radiation

I. INTRODUCTION

The need to develop new, clean, and efficient synthesis is on demand nowadays, in particular those associated with the direct mixture of reactants without a solvent because they avoid unwanted contaminants, making these methodologies less harmful to the ambient. The solvent-free preparation of products of different natures has been reported (Tanaka, 2003); in the case of the formation of C-N bonds, Wenz *et al.* (1997) prepared polyamides from α , ω -amino acids contained as inclusion compounds in α -cyclodextrin by the heating of the microcrystalline powder at temperatures above 473 K. Recently, Vouyiouka *et al.* (2005) proposed kinetic models to explain polyamide solid-state polymerization of nylon 6.6 resins by heating at temperatures of 433 to 473 K. Furthermore, the condensation product of the direct mixture of carboxylic acids and primary amines is amides; reactions of this type have been recently carried out using microwave irradiation (Perreux *et al.*, 2002). On the basis of these works, we proposed the direct conversion of N-carbamoyls to hydantoins by heating of reagent at certain temperature. Hydantoins or imidazolidine-2,4-diones are compounds with an imidazolic ring that have keto groups in positions 2 and 4. Depending on the nature and type of substitution on the heterocyclic ring, these compounds may display pharmaceutical and biological activity with a variety of applications: fungicidal (Marton *et al.*, 1993), antiviral (Opačić *et al.*, 2005), herbicide (Hanessian *et al.*, 1995), antitumoral and anti-inflammatory (Thenmozhiyal *et al.*, 2004), protein inhibitor (Wu *et al.*, 2004), HIV protease inhibitor (Comber *et al.*,

1992), hypolipidemic agent (Tompkins, 1986), and antihypertensive agent (Kieć-Kononowicz *et al.*, 2003). However, hydantoins are better known as anticonvulsants (Merritt and Putnam, 1938); if they are substituted by aliphatic groups they display hypnotic properties, while those substituted by phenyl groups, such as diphenylhydantoin, display antiepileptic activity (Cameron and Cameron, 1971; Thenmozhiyal *et al.*, 2004). Poupaert *et al.* (1984) and Cortes *et al.* (1985) observed a reduction on the anticonvulsant activity in 5,5-diphenylhydantoin when the imidazolidin-2,4-dione ring was compared with analogous compounds with imidazol-2-one and 2-thioxoimidazolidin-4-one rings. The reduction of the biological activity was attributed to alteration of the hydrogen donor and acceptor capacity of the heterocyclic rings. Recently, the biocatalytic conversion of hydantoins has called the attention since it is a source for production of natural and non-natural amino acids. The reaction involves two consecutive hydrolysis catalyzed by two enzymes: (1) dihydropyrimidase (EC 3.5.2.2), which converts 5-monosubstituted hydantoins into L- or D-N-carbamoyls; (2) N-carbamoylase (EC 3.5.1), which converts the L- or D-N-carbamoyls into L- or D- α -amino acids (Burton and Dorrington, 2004).

Here, we report the conversion of N-carbamoyl-L-proline to hydantoin-L-proline by direct heating at 470 K. The melt product was allowed to solidify and the crystal structure of hydantoin-L-proline was solved and refined from powder synchrotron diffraction data.

II. EXPERIMENTAL

A. Synthesis

Hydantoin-L-proline (II) was obtained from N-carbamoyl-L-proline (I) by the solvent-free reaction de-

^{a)}Electronic mail: asiloe@ula.ve

^{b)}Electronic mail: gerzon@ula.ve

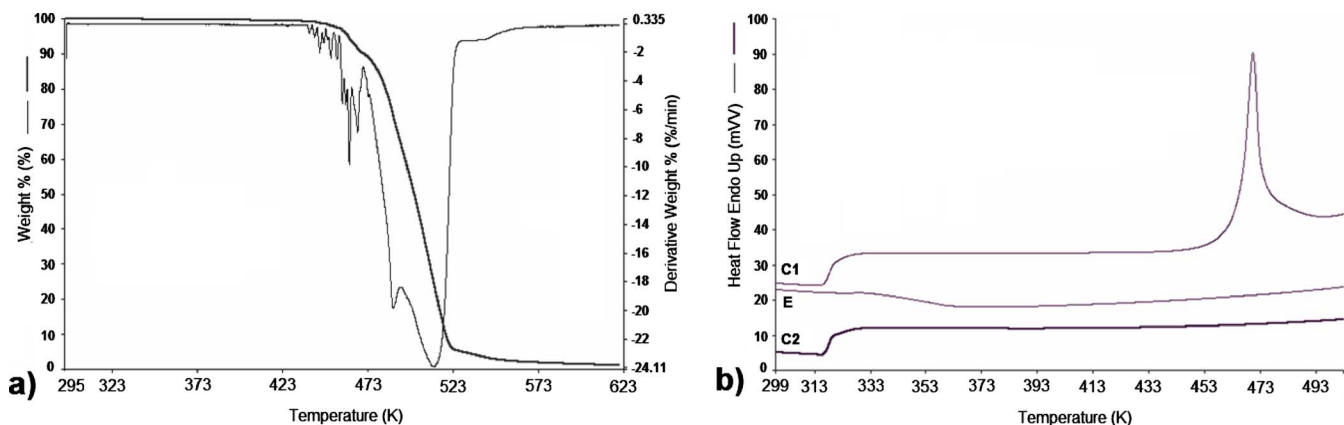


Figure 1. (Color online) (a) TGA plot of N-carbamoyl-L-proline; (b) DSC plot of N-carbamoyl-L-proline.

scribed here. The N-carbamoyl (I) (mp of 476 to 478 K) was obtained from L-proline following a synthetic procedure described elsewhere (Seijas *et al.*, 2006). FT-IR has 1695.5 cm^{-1} [t, C=O (acid group)] and 1660.8 cm^{-1} [t, C=O (carbamyl group)]. ^1H NMR has (400 MHz, DMSO- d_6) $\delta=12.45$ (b-s, H2), 5.88 (s, H2A, H2B), 4.14 (dd, H4), 3.32 (m, H1B), 3.23 (m, H1A), 1.84 (m, H3A), 2.06 (m, H3B), and 1.84 (H2C and H2D). ^{13}C NMR has (100.6 MHz, DMSO- d_6) $\delta=7$ (C5), 157.2 (C6), 58.4 (C4), 46.4 (C1), 29.6 (C3), and 24.4 (C2). 200 mg (1.266 mmol) of (I) was placed on a glass reactor under reduce pressure; the reactor was heated at a rate of $5^\circ/\text{min}$ from room temperature to 476 K, keeping the reactor at this temperature for 10 min until the complete fusion of the solid. The melt was allowed to cool to room temperature observing a change in the color of the solid from white to beige (yielding 98.0 mg, 0.700 mmol, and mp of 457 to 458 K). FT-IR has (in KBr Pallets) 3443 cm^{-1} (t, N-H), 1757 cm^{-1} (tsym, C=O), 1708 cm^{-1} (tasym, C=O), and 1405 cm^{-1} (t, C-N). ^1H NMR has (400 MHz, DMSO- d_6) $\delta=10.4$ (H3, b-s), 4.07 (H5A, t, J1 = 4 Hz), 3.43 (H8B, m), 3.02 (H8A, m), 3.23 (H1A, m), 1.95 (H7A=H7B m), 2.03 (H6B, m), and 1.60 (H6A, m); ^{13}C NMR has (100.6 MHz, DMSO- d_6) $\delta=161.0$ (C2), 175.4 (C4), 64.0 (C5), 44.9 (C8), 26.7 (C6), and 26.6 (C7). Additional signals in the ^1H NMR with very low intensity were observed at 1.75, 3.25, and 3.75 ppm.

B. Thermal analysis

For the thermogravimetric analysis, sufficient quantities of N-carbamoyl-L-proline (I) (4.1 mg) and hydantoin-L-proline (II) (5.3 mg) were placed on the aluminum canisters of a thermobalance Perkin-Elmer TGA7 programmed to heat

the samples from 295 to 623 K at a rate of 10 K min^{-1} under a dry N_2 flux of 50 mL min^{-1} . The thermograms for (I) were recorded and are shown in Figure 1.

C. Synchrotron X-ray powder diffraction

X-ray powder diffraction data of (I) and (II) were collected with the high-resolution X-ray powder diffractometer on beamline ID31, ESRF (Fitch, 2004), selecting X-rays from an undulator source with wavelengths of 0.799 93(1)\ \AA . Small quantities of (I) and (II) were lightly ground with a pestle in an agate mortar and introduced into 1.0-mm-diameter borosilicate glass capillaries, mounted on the axis of the diffractometer and spun at approximately 1 Hz during measurements. Data were collected in continuous mode, normalized against monitor counts and detector efficiencies, and rebinned into steps of $2\theta=0.003^\circ$.

III. RESULTS AND DISCUSSION

Figure 1(a) shows the TGA plot of (I). A weight loss of 10.6% occurs around 470 to 473 K, which can be explain as shown in Figure 2: (a) loss of a H_2O molecule, corresponding to the formation of tetrahydro-pyrrol-[1,2-c]-imidazol-1,3-dione or hydantoin-L-proline (IIa); (b) loss of a NH_3 molecule, which will produce the tetrahydro-pyrrol-[1,2-c]-oxazol-1,3-dione (IIb); or (c) both thermal reactions occurs simultaneously. Additional decomposition peaks are also seen at 489 and 530 K. The DSC plot [Figure 1(b)] of (I) shows the melting and decomposition peaks overlapping at 470.7 K. Also, the baseline of the DSC rises prior to melting, which is an evidence of the onset of the thermal reaction Iia

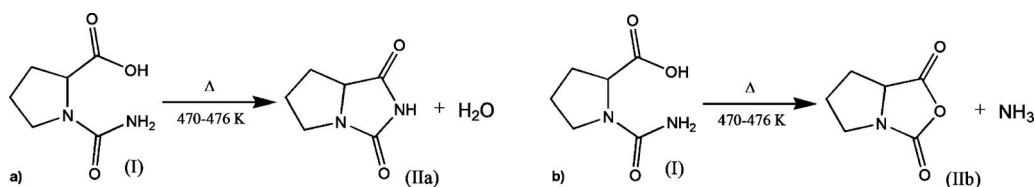


Figure 2. Two possible reaction routes for the thermal decomposition of N-carbamoyl-L-proline (i) at 473 K. Cyclization of (i) to form an imidazol ring (IIa) and water (left). Cyclization of (i) to form an oxazol ring (IIb) and ammonia (right). Both reactions explain a weight loss of around $10 \pm 2\%$ in the TGA experiment.

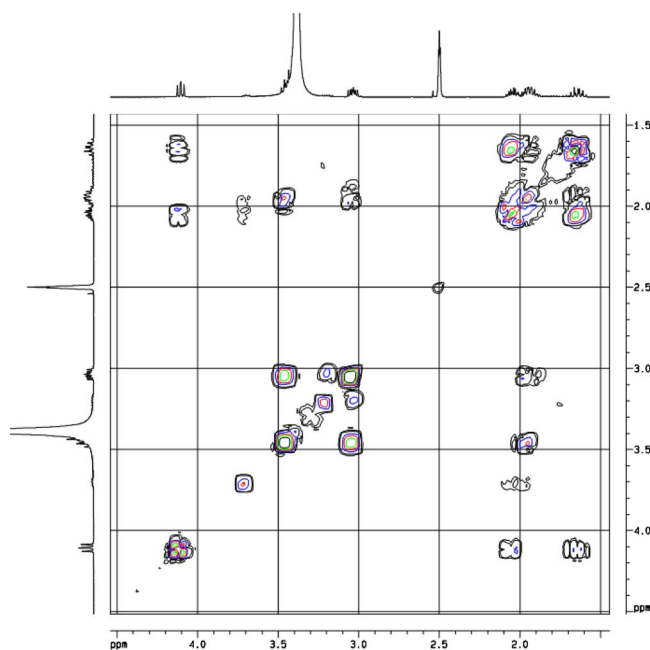


Figure 3. (Color online) ^1H - ^1H COSY spectra of the reaction product.

or IIb, which changes the nature of the compound and hence its molar heat capacity (C_p). The ^1H NMR spectra of the thermal reaction product show all the signals corresponding to compound IIa and few additional peaks of very low intensity, which could be assigned to another unidentified compound present in the reaction bulk in very small quantities. In the ^1H - ^1H COSY spectra, these additional signals are more clearly observed, and since they are all correlated with each other, it can be inferred that all of them belong to a single compound (see Figure 3).

The powder diffraction pattern of the starting reactive N-carbamoyl-L-proline (I) is shown in Figure 4(a). It was indexed in an $P2_12_12_1$ orthorhombic cell, with cell parameters $a=6.4704(1)$ Å, $b=9.7644(1)$ Å, and $c=12.5135(2)$ Å (refined values) [DICVOL04 (Boultif and Louër, 2004), $M_{(20)}=99.7$ (de Wolff, 1968), and $F_{(20)}=373.7$ (Smith and Snyder, 1979)]. The cell parameters match those reported by Seijas *et al.* (2007) from a single crystal study, and therefore a Rietveld refinement of the diffraction pattern was carried out using the structure reported by those authors; also, no additional phases were observed in it. The diffraction pattern of the reaction product shown in Figure 4(b) was indexed in an orthorhombic cell, with cell parameters $a=11.37653(3)$ Å, $b=8.00112(2)$ Å, and $c=7.13916(2)$ Å (refined values) [DICVOL04 (Boultif and Louër, 2004), $M_{(20)}=1267.6$ (de Wolff, 1968), and $F_{(20)}=3877.7$ (Smith and Snyder, 1979)]. The diffraction pattern showed eight additional peaks of very low intensity belonging to the unidentified compound also observed in the NMR experiments. Neither the NMR nor the diffraction experiment allowed the identification of the spurious phase, which might possibly be the product of the second reaction proposed in scheme 1. Evaluation of the systematic absent reflections of the major phase yielded space group $P2_12_12_1$ (No. 19). The structural solution was carried out using the simulated annealing program DASH (David *et al.*, 2006). The

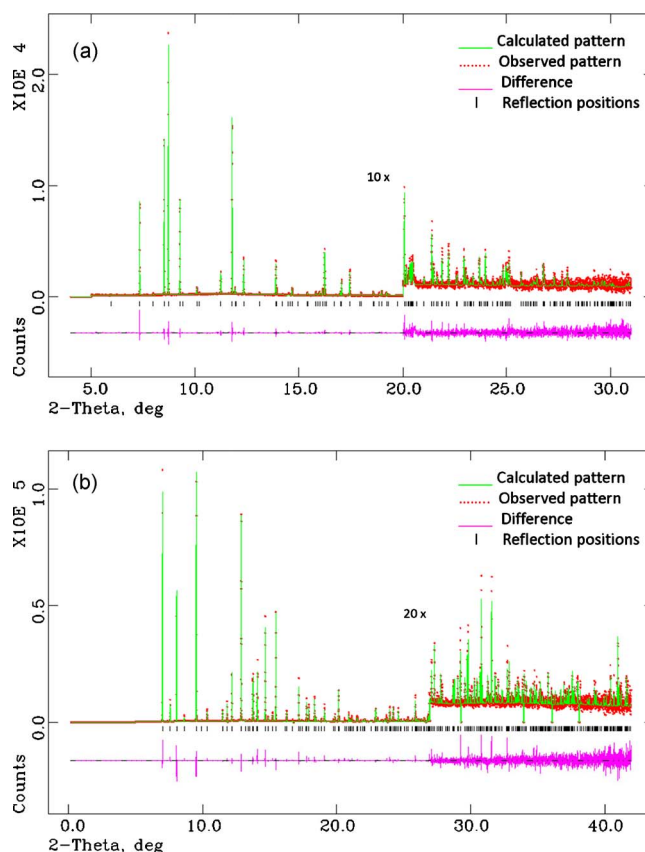


Figure 4. (Color online) Final Rietveld plot for (a) N-carbamoyl-L-proline (I) and (b) hydantoin-L-proline (IIa).

starting molecule for the simulated annealing was obtained using the *ab initio* RHF/6-311G orbital optimization calculations implemented in GAUSSIAN03 (Frisch *et al.*, 2003). Cycles of ten million moves were performed and the program afforded a solution χ^2 of 16.4.

The model was refined against the diffraction pattern using the Rietveld method (Rietveld, 1969) implemented in the program GSAS (Larson and Von Dreele, 2004). Data in the range from 5° to 41.973° 2θ comprising 310 reflections were modeled with a pseudo-Voigt peak shape function (Thompson *et al.*, 1987), which includes the axial divergence correction at low angle (Finger *et al.*, 1994). The background was described by the automatic linear interpolation of 20 points throughout the diffraction pattern. Restraints were applied to bond distance and bond angles with weights being 0.001–0.005 Å and 1° , respectively. The restrained values for bond distances and angles were taken from the structure obtained by the *ab initio* RHF/6-311G calculations. The thermal motion was refined as follows: (a) an overall isotropic temperature factor for all the nonhydrogen atoms and (b) temperature factors for hydrogen atoms taken as 1.2 times the value of the nonhydrogen atoms. In the final Rietveld cycles the eight diffraction peaks corresponding to traces of the secondary unindexed phase were excluded from the pattern, improving the figures of merit by 3%. Details of the diffraction experiment, structural solution, and Rietveld refinement are summarized in Table I. Experimental, calculated, and differences plot for the final refinement cycle for compound (I) and (IIa) are shown in Figure 4. Table II shows

TABLE I. Crystallographic data and experimental details.

	(I)	(IIa)
Crystal data		
Chemical formula	C ₆ H ₁₀ O ₃ N ₂	C ₆ H ₈ O ₂ N ₂
M_r	158.07	140.06
Cell setting, space group	Orthorhombic, $P2_12_12_1$	Orthorhombic, $P2_12_12_1$
Temperature (K)	295	295
a, b, c (Å)	6.470 79 (7), 9.765 45 (7), 12.5142 (1)	11.376 82 (2), 8.001 34 (1), 7.139 39 (1)
V (Å ³)	790.77 (2)	649.90 (2)
Z	4	4
D_x (Mg m ⁻³)	1.325	1.432
Radiation type	Synchrotron	Synchrotron
Incident radiation wavelength (Å)	0.799 93	0.799 93
μ (mm ⁻¹)	0.11	0.048
Specimen form, color	Cylinder (particle morphology: thin powder), white	Cylinder (particle morphology: thin powder), beige
Specimen size (mm)	1.5 × 40	1.5 × 40
Specimen preparation temperature (K)	Room temperature	Room temperature
Data collection		
Diffractometer	Beamline ID31, ESRF	Beamline ID31, ESRF
Data collection method	Specimen mounting: borosilicate glass capillary; mode: transmission; scan method: continuous	Specimen mounting: borosilicate glass capillary; mode: transmission; scan method: continuous
Absorption correction	None	None
2θ (deg)	2θ min=4.002, 2θ max=31.82, increment=0.003	2θ min=5.00, 2θ max=41.97, increment=0.003
Refinement		
R -factors: R_p, R_{wp}, R_{exp}	0.0885, 0.1235, 0.06920	0.0876, 0.1223, 0.0379
Wavelength of incident radiation (Å)	0.799 93	0.799 93
Excluded region(s)	None	Eight; 11.832 to 11.859, 16.749 to 16.815, 23.796 to 23.841, 26.661 to 26.700, 29.268 to 29.316, 33.921 to 33.954, 36.048 to 36.084, 38.064 to 38.136
Profile function	CW profile function number 4 with 19 terms	CW profile function number 4 with 19 terms
No. of parameters	98	93
$(\Delta/\sigma)_{max}$	0.04	0.05

a selection of bond distances and angles for compound (IIa).

The analysis of the hydrogen bond network of N-carbamoyl-L-proline (I) (Seijas *et al.*, 2007) shows hydrogen bonds, two of the type N \cdots H \cdots O and one O \cdots H \cdots O. These hydrogen bonds lock both the ureide and the acidic groups in an orientation that makes the NH₂ group “anti” to the carboxylic acid group and at a distance of 4.310(3) Å from its carbonylic carbon; therefore, any nucleophilic attack from the lone pair of the NH₂ group to this carbon is geometrically hindered in the solid state. However, once the compound reaches its melting point, the free rotation of the ureide and the carboxylic acid groups is allowed and, therefore, a nucleophilic intramolecular substitution reaction might take place through the route shown in Figure 5 (Perreux *et al.*, 2002).

Once the reaction has taken place and the melt of the product solidifies, the molecular rearrangement caused by the reaction is so subtle that as a result the product (IIa) crystallizes in the same space group as the reactant (I), with more or less similar molecular packing but undergoing a cell contraction of 150 Å³ from the loss of four water molecules, one from each carbamoyl converted into the corresponding hydantoin in the unit cell. Figure 6 shows the molecular

structure of the hydantoin-L-proline (IIa) with the atom labeling scheme. Bond distances in the same hydantoin [structural report without hydrogen atoms (Arte *et al.*, 1980)] and other hydantoin rings (Yu *et al.*, 2004; Rizzi *et al.*, 1989; Gauthier *et al.*, 1997; Delgado *et al.*, 2007) show similar asymmetry patterns as the ones reported here, with bond distances N1–C2 and N3–C4 being shorter by 0.057 Å than N3–C2 bond distance. The asymmetry parameters of Griffin *et al.* (1984) evaluated in the pyrrolidin ring show an envelope conformation, with C1 being the flap of the envelope [$\Delta C_{s_{max}} = +47.1(3)^\circ$, $\Delta C_{s_{min}} = +1.9(4)^\circ$, $\Delta C2_{max} = +62.0(3)^\circ$, $\Delta C2_{min} = 16.5(3)^\circ$, $\Delta C_s(C1) = 1.9(4)^\circ$, and $\Delta C_s(C4-N3) = 1.9(4)^\circ$]. The crystal packing is stabilized by a hydrogen bond of the type N–H \cdots O and two of the type C–H \cdots O. The geometry of these hydrogen bonds is summarized in Table III. Pairs of molecules related by 2_1 screw axes interact by hydrogen bond N3–H3 \cdots O4 $[1-x, -\frac{1}{2}+y, \frac{1}{2}-z]$, forming supramolecular chain structure described by the graph set C(4) (Etter, 1990) (Figure 7). The repetition of these ribbons along a by means of another 2_1 screw axis produces sheets of molecules that pile up along the c direction. These sheets are linked by additional nonconventional hydrogen bonds of the

TABLE II. Selected bond distances (Å) and bond angles (deg) for hydantoin-L-proline (IIa).

	(IIa)	RHF/6-311G	Difference
N1–C2	1.349(4)	1.361	–0.012
C2–N5	1.421(4)	1.396	0.025
N5–C4	1.343(4)	1.373	–0.030
C4–C5	1.557(5)	1.513	–0.044
C5–N1	1.496(5)	1.461	0.035
C2–O2	1.220(3)	1.217	0.003
C4–O4	1.209(2)	1.213	–0.008
C5–C8	1.505(4)	1.524	–0.019
C8–C7	1.549(4)	1.546	0.003
C7–C6	1.539(4)	1.552	–0.013
C6–N1	1.508(4)	1.461	0.047
N1–C2–O1	127.1(3)	128.3	–1.2
N1–C2–N3	106.2(3)	106.0	0.2
N3–C2–O2	124.4(3)	125.7	–1.3
C2–N3–C4	115.9(2)	113.3	2.6
N3–C4–O4	128.3(4)	126.6	1.7
N3–C4–C5	104.4(2)	105.6	–1.2
C5–C4–O4	127.3(4)	127.7	–0.4
C4–C5–N1	103.6(3)	102.5	1.1
C2–N1–C5	109.8(3)	112.3	–2.5
C5–C8–C7	101.6(2)	102.1	–0.5
C8–C7–C6	105.9(2)	105.7	0.2
C7–C6–N1	104.0(2)	103.7	0.3
C6–N1–C5	111.4(3)	113.0	–1.6
N1–C5–C8	101.9(3)	102.8	–0.9

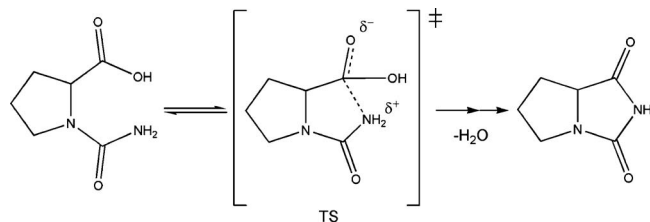


Figure 5. Mechanism for the intramolecular nucleophilic attack from the lone pair of the NH₂ group to the carboxylic acid group.

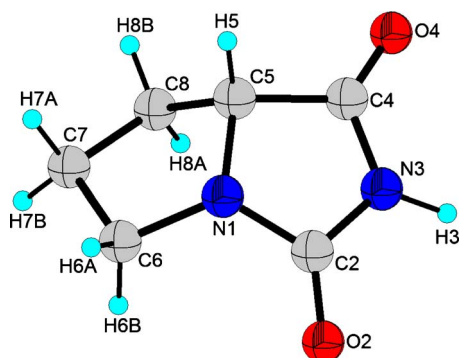


Figure 6. (Color online) Asymmetric unit and atom labeling scheme for the hydantoin-L-proline (IIa).

TABLE III. Hydrogen bonds in hydantoin-L-proline (IIa).

D–H···A	D–H (Å)	H···A (Å)	D···A (Å)	D–H···A (deg)
N3–H3···O4 ^a	0.970(3)	1.938(3)	2.903(3)	173.3(5)
C8–H8A···O2 ^b	0.990(3)	2.686(4)	3.602(3)	154.0(4)
C5–H5···O2 ^c	0.990(5)	2.556(3)	3.213(3)	123.7(3)

^aSymmetry code: $1-x, -\frac{1}{2}+y, \frac{1}{2}-z$.

^bSymmetry codes: $\frac{1}{2}-x, -y, -\frac{1}{2}-z$.

^cSymmetry codes: $\frac{1}{2}-x, -y, \frac{1}{2}+z$.

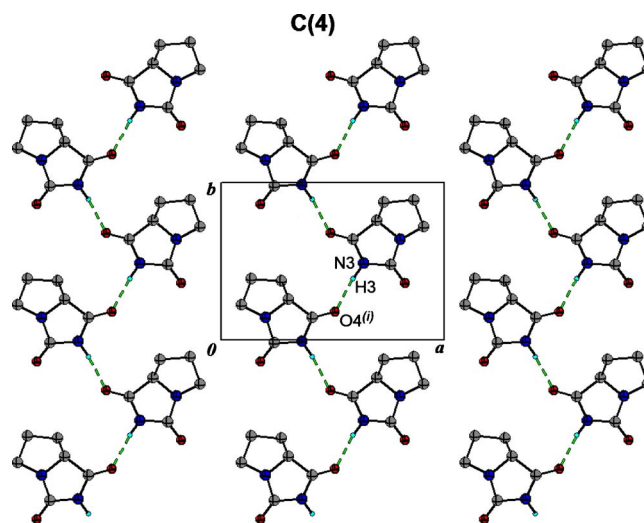


Figure 7. (Color online) Partial packing view along *c* of hydantoin-L-proline (IIa). Broken lines indicate the hydrogen bonds. H atoms not involved in hydrogen bonding have been omitted for clarity. [Symmetry code: (i) $1-x, -\frac{1}{2}+y, \frac{1}{2}-z$.]

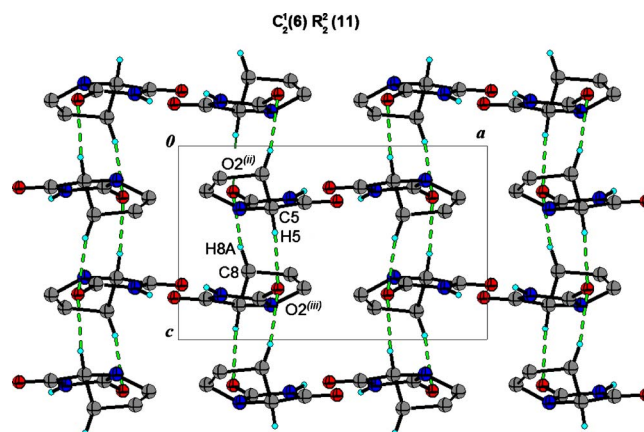


Figure 8. (Color online) Packing view along (*b*) of hydantoin-L-proline (IIa). Broken lines indicate the hydrogen bonds. H atoms not involved in hydrogen bonding have been omitted for clarity. [Symmetry codes: (ii) $\frac{1}{2}-x, -y, -\frac{1}{2}-z$; (iii) $\frac{1}{2}-x, -y, \frac{1}{2}+z$.]

type C–H···O, C8–H8A···O2 [$\frac{1}{2}-x, -y, -\frac{1}{2}-z$], and C5–H5···O2 [$\frac{1}{2}-x, -y, \frac{1}{2}+z$], forming chains of fused supramolecular rings described by the graph set $C_2^1(6)R_2^2$ as shown in Figure 8.

IV. CONCLUSION

Conversion of N-carbamoyl-L-proline to hydantoin-L-proline was studied by means of X-ray powder diffraction experiments. Solvent-free in the solid state hydantoin-L-proline was obtained from direct heating of N-carbamoyl-L-proline via a nucleophilic intramolecular substitution reaction at 470 K. For this compound, a supramolecular chain structure is formed with a crystal packing directed by hydrogen bonds which displays a layered structure pile up along the *c* direction.

ACKNOWLEDGMENTS

We thank beamline ID31, ESRF for providing synchrotron radiation beam time, the CDCHT-ULA (Grant Nos. C-1618-08-08-AA and C-1614-08-08-B), and FONACIT (Grant No. LAB-97000821).

Arte, E., Tinant, B., Declercq, J., Germain, G., and van Meerssche, M. (1980). "Structure of 2 proline hydantoin derivatives l-proline hydantoin and d-allohydroxyproline hydantoin," *Bull. Soc. Chim. Belg.* **89**, 379–384.

Boultif, A. and Louër, D. (2004). "Powder pattern indexing with the dichotomy method," *J. Appl. Crystallogr.* **37**, 724–731.

Burton, S. G. and Dorrington, R. A. (2004). "Hydantoin-hydrolysing enzymes for the enantioselective production of amino acids: New insights and applications," *Tetrahedron: Asymmetry* **15**, 2737–2741.

Camerman, A. and Camerman, N. (1971). "The stereochemical basis of anticonvulsant drug action. I. The crystal and molecular structure of diphenylhydantoin, a noncentrosymmetric structure solved by centric symbolic addition," *Acta Crystallogr., Sect. B: Struct. Crystallogr. Cryst. Chem.* **27**, 2205–2211.

Comber, R. N., Reynolds, C. R., Friedrich, J. D., Manguikian, R. A., Buckheit, R. W., Truss, J. W., Shannon, W. M., and Secrist, J. A. (1992). "5,5-disubstituted hydantoins—Syntheses and anti-HIV activity," *J. Med. Chem.* **35**, 3567–3572.

Cortes, S., Liao, Z. K., Watson, D., and Kohn, H. (1985). "Effect of structural modification of the hydantoin ring on anticonvulsant activity," *J. Med. Chem.* **28**, 601–606.

David, W. I. F., Shankland, K., van de Streek, J., Pidcock, E., Motherwell, W. D. S., and Cole, J. C. (2006). "DASH: A program for crystal structure determination from powder diffraction data," *J. Appl. Crystallogr.* **39**, 910–915.

Delgado, G. E., Mora, A. J., Uzcátegui, J., Bahsas, A., and Briceño, A. (2007). "(S)-5-benzylimidazolidine-2,4-dione monohydrate," *Acta Crystallogr., Sect. C: Cryst. Struct. Commun.* **63**, o448–o450.

de Wolff, P. M. (1968). "A simplified criterion for the reliability of a powder pattern indexing," *J. Appl. Crystallogr.* **1**, 108–113.

Etter, M. C. (1990). "Encoding and decoding hydrogen-bond patterns of organic-compounds," *Acc. Chem. Res.* **23**, 120–126.

Finger, L. W., Cox, L. W., and Jephcoat, A. P. (1994). "A correction for powder diffraction peak asymmetry due to axial divergence," *J. Appl. Crystallogr.* **27**, 892–900.

Fitch, A. N. (2004). "The high resolution powder diffraction beam line at ESRF," *J. Res. Natl. Inst. Stand. Technol.* **109**, 133–142.

Frisch, M. J., Trucks, G. W., Schlegel, H. B., Scuseria, G. E., Robb, M. A., Cheeseman, J. R., Montgomery, J. A., Vreven, T., Jr., Kudin, K. N., Burant, J. C., Millam, J. M., Iyengar, S. S., Tomasi, J., Barone, V., Mennucci, B., Cossi, M., Scalmani, G., Rega, N., Petersson, G. A., Nakatsuji, H., Hada, M., Ehara, M., Toyota, K., Fukuda, R., Hasegawa, J., Ishida, M., Nakajima, T., Honda, Y., Kitao, O., Nakai, H., Klene, M., Knox, J. E., Hratchian, H. P., Cross, J. B., Bakken, V., Adamo, C.,

Jaramillo, J., Gomperts, R., Stratmann, R. E., Yazyev, O., Austin, A. J., Cammi, R., Pomelli, C., Ochterski, J. W., Ayala, P. Y., Morokuma, K., Voth, G. A., Salvador, P., Dannenberg, J. J., Zakrzewski, V. G., Dapprich, S., Daniels, A. D., Strain, M. C., Farkas, O., Malick, D. K., Rabuck, A. D., Raghavachari, K., Foresman, J. B., Ortiz, J. V., Cui, Q., Baboul, A. G., Clifford, S., Cioslowski, J., Stefanov, B. B., Liu, G., Liashenko, A., Piskorz, P., Komaromi, I., Martin, R. L., Fox, D. J., Keith, T., Al-Laham, M. A., Peng, C. Y., Nanayakkara, A., Challacombe, M., Gill, P. M. W., Johnson, B., Chen, W., Wong, M. W., Gonzalez, C., and Pople, J. A. (2003). GAUSSIAN03, Revision B. 02 (Computer Software), Gaussian, Inc., Wallingford, CT.

Gauthier, T., Yokum, T., Morales, G., McLaughlin, M., Liu, Y., and Fronczek, F. (1997). "Two cyclohexanespiro-5'-hydantoin monohydrates," *Acta Crystallogr., Sect. C: Cryst. Struct. Commun.* **53**, 1659–1661.

Griffin, J. F., Duax, W., and Weeks, M. (1984). *Atlas of Steroid Structure* (Plenum Publishing Corporation, New York).

Hanessian, S., Sanceau, J. Y., and Chemla, P. (1995). "Synthesis of surrogate structures related to the herbicidal agent hydantocidin," *Tetrahedron* **51**, 6669–6678.

Kieć-Kononowicz, K., Stadnicka, K., Mitka, A., Pękala, E., Filipek, B., Sapa, J., and Zygmunt, M. (2003). "Synthesis, structure and antiarrhythmic properties evaluation of new basic derivatives of 5,5-diphenylhydantoin," *Eur. J. Med. Chem.* **38**, 555–566.

Larson, A. C. and Von Dreele, R. B. (2004). General Structure Analysis System (GSAS), Report LAUR 86-748, Los Alamos National Laboratory, Los Alamos, NM.

Marton, J., Enisz, J., Hosztafi, S., and Timar, T. (1993). "Preparation and fungicidal activity of 5-substituted hydantoins and their 2-thio analogs," *J. Agric. Food Chem.* **41**, 148–152.

Merrit, H. H. and Putnam, T. J. (1938). "A new series of anticonvulsant drugs tested by experiments on animals," *Schweiz Arch. Neurol. Psychiatr.* **39**, 1003–1015.

Opacić, N., Barbarić, M., Zorc, B., Cetina, M., Nagl, A., Frković, D., Kralj, M., Pavelić, K., Balzarini, J., Andrei, G., Snoeck, R., De Clercq, E., Raić-Malić, S., and Mintas, M. (2005). "The novel L- and D-amino acid derivatives of hydroxyurea and hydantoins: Synthesis, X-ray crystal structure study, and cytostatic and antiviral activity evaluations," *J. Med. Chem.* **48**, 475–482.

Perreux, L., Loupy, A., and Volatron, F. (2002). "Solvent-free preparation of amides from acids and primary amines under microwave irradiation," *Tetrahedron* **58**, 2155–2162.

Poupaert, J. H., Vandervorst, D., Guiot, P., Mustafa, M. M., and Dumont, P. (1984). "Structure activity relationships of phenytoin-like anticonvulsant drugs," *J. Med. Chem.* **27**, 76–78.

Rietveld, H. M. (1969). "A profile refinement method for nuclear and magnetic structures," *J. Appl. Crystallogr.* **2**, 65–71.

Rizzi, J. P., Schnur, R., Hutson, N., Kraus, K., and Kelbaugh, P. (1989). "Rotationally restricted mimics of rigid molecules—Nonspirocyclic hydantoin aldose reductase inhibitors," *J. Med. Chem.* **32**, 1208–1213.

Seijas, L. E., Delgado, G. E., Mora, A. J., Bahsas, A., and Briceño, A. (2007). "(2S)-l-carbamoylpyrrolidine-2-carboxylic acid," *Acta Crystallogr., Sect. C: Cryst. Struct. Commun.* **63**, o303–o305.

Seijas, L. E., Delgado, G. E., Mora, A. J., Bahsas, A., and Uzcátegui, J. (2006). "Síntesis y caracterización de los derivados N-carbamilo de hidantoína de L-prolina," *Avances en Química* **1**, 3–7.

Smith, G. S. and Snyder, R. L. (1979). " F_N : A criterion for rating powder diffraction patterns and evaluating the reliability of powder-pattern indexing," *J. Appl. Crystallogr.* **12**, 60–65.

Tanaka, K. (2003). *Solvent-Free Organic Synthesis* (Wiley-VCH Verlag GmbH and Co. KGaA, Weinheim).

Thenmozhiyal, J. C., Wong, P. T., and Chui, W.-K. (2004). "Anticonvulsant activity of phenylmethylenehydantoins: A structure-activity relationship study," *J. Med. Chem.* **47**, 1527–1535.

Thompson, P., Cox, D., and Hastings, J. B. (1987). "Rietveld refinement of Debye-Scherrer synchrotron X-ray data from Al₂O₃," *J. Appl. Crystallogr.* **20**, 79–83.

Tompkins, E. (1986). "5,5-diaryl-2-thiohydantoins and 5,5-diaryl-n-3-substituted-2-thio hydantoins as potential hypolipidemic agents," *J. Med. Chem.* **29**, 855–859.

Vouyiouka, S. N., Karakatsani, E. K., and Pappaspyride, C. D. (2005). "Solid state polymerization," *Prog. Polym. Sci.* **30**, 10–37.

Wenz, G., Steinbrunn, M. B., and Landfester, K. (1997). "Solid state polycondensation within cyclodextrin channels leading to water soluble polyamide rotaxanes," *Tetrahedron* **53**, 15575–15592.

- Wu, J. P., Emeigh, J., Gao, D. H. A., Goldberg, D. R., Kuzmich, D., Miao, C., Potocki, I., Qian, K. C., Sorcek, R. J., Jeanfavre, D. D., Kishimoto, K., Mainolfi, E. A., Nabozny, G., Peng, C., Reilly, P., Rothlein, R., Sellati, R. H., Woska, J. R., Chen, S., Gunn, J. A., O'Brien, D., Norris, S. H., and Kelly, T. A. (2004). "Second-generation lymphocyte function-associated antigen-1 inhibitors: 1H-imidazo[1,2-alpha]imidazol-2-one derivatives," *J. Med. Chem.* **47**, 5356–5366.
- Yu, F., Schwalbe, C. H., and Watkin, D. (2004). "Hydantoin and hydrogen-bonding patterns in hydantoin derivatives," *Acta Crystallogr., Sect. C: Cryst. Struct. Commun.* **60**, o714–o717.